Photoreflectance of 0.4-nm single-walled carbon nanotubes

C. L. Yang, B. Hou, Irene L. Li, Z. M. Li, Z. K. Tang, J. N. Wang, H. J. Liu, and W. K. Ge*
Department of Physics and Institute of Nano-Science and Technology, Hong Kong University of Science and Technology, Clear Water Bay, Kowloon, Hong Kong, China
(Received 14 September 2004; revised manuscript received 14 January 2005; published 23 June 2005)

The photoreflectance spectra of the 0.4-nm diameter single-walled carbon nanotubes (SWNTs) have been measured. The sharp features obtained from the experimental spectra have been identified to be the van Hove singularities associated with tubes of different chiralities, and fitted by the first-order derivatives of both real and imaginary parts of the dielectric functions, such that the band structures of the SWNTs are further clarified.

DOI: 10.1103/PhysRevB.71.233404 PACS number(s): 78.67.Ch, 73.22.−f

I. INTRODUCTION

Single-walled carbon nanotubes (SWNTs) with diameter as small as 0.4 nm, composed of three chiralities (3, 3), (4, 2), and (5, 0), have been produced in $AlPO_4$-5 zeolite single crystals.[1] The uniformity of their size and the consistency of their alignment in the 1-nm-sized channels of $AlPO_4$-5 facilitate the experimental investigation of optical properties of SWNTs. The polarized optical absorption spectra of the 0.4 -nm SWNTs have been measured, and their band structures and dielectric functions have been calculated from local density function approximation (LDA) considering of the curvature effect to understand the characteristics in the absorption spectra.[2,3] There was, however, a discrepancy between the theoretical calculation and the experimental measurement. The van Hove singularities in the imaginary parts of the calculated dielectric functions were not entirely identified in the absorption spectra, where some features were very weak. In the past years, excitonic effects in small-sized carbon nanotubes have drawn more and more attention, since exciton binding energy due to the long-range Coulomb interaction is expected to become significant in one-dimensional (1D) system.[4–7] It has also been found that the short-range electron-electron interactions play a vital role in the carbon nanotubes. Recent theoretical developments[8] concerning the many-electron effects in SWNTs predicted bound exciton states in some semiconducting and metallic nanotubes. While it was pointed out that the electron-hole interaction could be governed by a repulsive exchange term for the (5, 0) tube where the symmetry of the bands prohibits direct attraction between the electon-hole pairs. So more detailed and precisely experimental determination of the optical transitions in SWNTs will be beneficial to understand more about their electronic structures and excitonic effects.

As an important tool to study electron-hole interactions and excitonic effects, modulation spectroscopy may provide more information about the optical transitions in materials than the absorption spectra, because it produces sharp and derivativelike features of primary spectrum.[9,10] Electroreflectance (ER) and photoreflectance (PR) measurements are two forms of modulation spectroscopy techniques and have been extensively used for characterizing the properties of quasizero, two- and three-dimensional materials in the last few decades. In PR, the modulation is achieved by a chopped pumping laser beam, which makes PR a contactless and nondestructive technique with broader applications. In this Brief Report, we performed the PR measurement of the 0.4-nm SWNTs and also the line shape analysis of the modulated reflectance spectra. An additional peak in comparison with the absorption spectra was observed, owing to the advantage of the PR spectra. All the van Hove singularities in the density of states were thereby recognized in the PR spectra within the measured energy range. Sharp features as narrow as 5 meV were resolved and the transition energies in the SWNTs were more accurately determined. Based on the comparison between the experimental results and the LDA calculation, the excitonic and many-electron effects in the 0.4-nm SWNTs were discussed.

II. PHOTOREFLECTANCE MEASUREMENT

Room-temperature modulated photoreflectance spectra were measured using a microscopic PR system (with focus about 10 μm). A 488-nm Ar^+ laser source, which was polarized parallel to the axis of the SWNTs and chopped at 300 Hz, was used as the pumping beam. The monochromatic probe beam (unpolarized) from a tungsten lamp was dispersed by a 0.25 m monochromator. The back reflected probe light from the sample surface was detected by a silicon photodetector with a lock-in amplifier, as schematically shown in the upper diagram of Fig. 1. The photo of the sample, which was a SWNT-filled zeolite crystal in yellow-brown color, was also presented in the diagram to show what we were dealing with. For pure zeolite without carbon nanotubes, there is no feature in the PR or absorption spectra from near infrared to ultraviolet.

The PR spectrum of the 0.4-nm SWNTs in the energy range from 1.1 to 2.7 eV is shown in Fig. 1, where three features were denoted as A, B, and A'. These features originated from the van Hove singularities of the density of states in the energy bands of the SWNTs. Two of them, A and B, have been detected in the absorption curve[2] as plotted at the bottom of Fig. 1, but A' fails to be resolved, which we suggest is due to both the smaller density of states and the suppression of this transition by the electron-hole exchange interaction.[8] The PR feature A' is associated with the minor peak of the imaginary part of the dielectric function for the (5, 0) tube, judging from its energy position.[3]

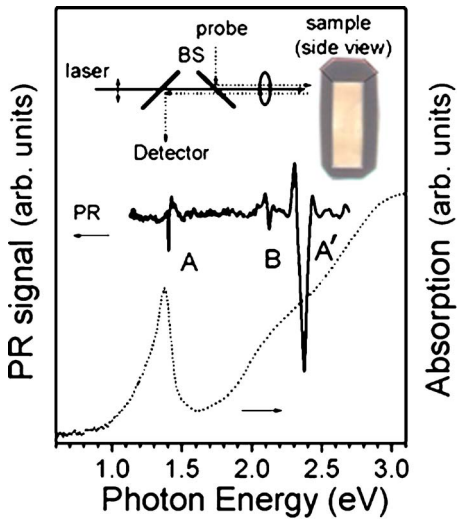

FIG. 1. The photoreflectance spectrum (solid line) from a bundle of the 0.4-nm SWNTs. The absorption spectrum (dotted line) is drawn at the bottom for comparison. The upper inset is the schematic diagram of the PR measurement setup. BS is short for beam splitter. The illustrated sample is a photo taken from the side view of a hexagonal zeolite crystal filled with SWNTs.

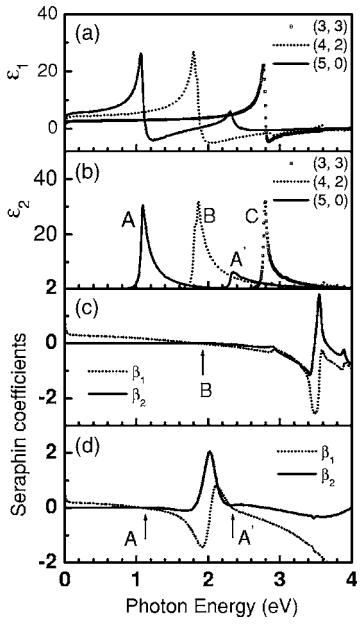

FIG. 2. The (a) real part ε_1 and (b) imaginary part ε_2 of the dielectric functions of three chiralities of SWNTs from the Liu and Chan calculation (Ref. 3). The Seraphin coefficients of the (4, 2) and (5, 0) tubes are plotted in the (c) and (d) panels, respectively.

III. EXPLANATION AND DISCUSSION

Since no work on PR in such a 1D system has ever been reported, the underlying modulation mechanism for the PR of the carbon nanotubes will be of fundamental interest. The PR effect is usually coming from an optical modulation of the dielectric function by the change in the surface electric field, by free carrier screening of excitons or by thermal heating effect.[11] We believe that the modulation of the surface electric field for SWNTs will not be a contribution since the electron movement or the depletion effect cannot occur along the radial direction or toward the tube surface. Though the thermal heating effect cannot be excluded from the modulation, we believe it plays a minor role here. The transparent zeolite template dominates the weight of our sample[12] and as a result presents a large heat reservoir for the carbon tubes inside, which reduces the photomodulated temperature variation of the SWNTs. If the energy relaxation process by the efficient light emission from the nanotubes[13] is further taken into account, then the temperature variation will become even smaller. So the thermal modulation, which is proportional to the temperature change, is unexpected to be significant here. Since the excitonic effects are demonstrated to be strong in the ultra-small nanotubes, the modulation based on the excitonic screening by the photogenerated carriers is thereby suggested to be the dominant mechanism.

The normalized differential change in the reflectivity measured in the PR experiment can be related to the perturbation of the complex dielectric function ($\varepsilon=\varepsilon_1+i\varepsilon_2$) and expressed as

$$\frac{\Delta R}{R} = \beta_1 \Delta\varepsilon_1 + \beta_2 \Delta\varepsilon_2, \tag{1}$$

where β_1 and β_2 are the Seraphin coefficients, and $\Delta\varepsilon_1$ and $\Delta\varepsilon_2$ are the changes in the real and imaginary parts of the dielectric function resulting from a change in the intensity of the pump beam F. The Seraphin coefficients β_1 and β_2 are related to the unperturbed dielectric function according to the formula[14]

$$\beta_1 = \frac{\partial \ln R}{\partial \varepsilon_1} = C_1[(\varepsilon_1 - 1)A_+ + \varepsilon_2 A_-], \tag{2}$$

$$\beta_2 = \frac{\partial \ln R}{\partial \varepsilon_2} = C_2\left[\frac{(\varepsilon_1 - 1)}{A_+} - \frac{\varepsilon_2}{A_-}\right], \tag{3}$$

with $A_\pm = \pm\sqrt{2}(\sqrt{\varepsilon_1^2+\varepsilon_2^2} \pm \varepsilon_1)^{1/2}/\sqrt{\varepsilon_1^2+\varepsilon_2^2}$, $C_1 = 1/(\varepsilon_1-1)^2+\varepsilon_2^2$, and $C_2 = 2\varepsilon_2/[(\varepsilon_1-1)^2+\varepsilon_2^2](\varepsilon_1^2+\varepsilon_2^2)$. Taking the theoretical dielectric functions of these tubes,[3] as shown in Figs. 2(a) and 2(b), the spectral dependence of β_1 and β_2 of the tubes (4, 2) and (5, 0) is calculated and plotted in Figs. 2(c) and 2(d). As β_2 is nearly zero at the lowest optical transitions A and B for the tubes (5, 0) and (4, 2), respectively, the PR spectrum at these two energies comes mainly from the modulation of ε_1, i.e., $\Delta R/R \cong \beta_1 \Delta\varepsilon_1$. This is similar to the case of PR around the fundamental absorption edge for bulk semiconductors as well as quantum well structures. Around the energy of the peak A', however, β_2 dominates and therefore the PR signal is contributed mostly from the modulation of ε_2, i.e., $\Delta R/R \cong \beta_2 \Delta\varepsilon_2$. Based on the criteria discussed here, we can determine whether the modulation comes dominatingly from the change in the real or imaginary part of their dielectric functions for the following line shape analysis. In the line shape fitting, dielectric functions with Lorentzian profile are adopted at these peaks, which is appropriate to describe the sharp excitonic transitions.

We employed the line shape theory originally developed for the PR spectrum of excitons in multiple quantum wells (MQWs), considering both MQWs and SWNTs are confined systems with exciton wave functions localized in space. For the excitonic transitions, the change in the dielectric function induced by the modulating parameter F is in the first derivative functional form and formulated as

$$\Delta\varepsilon_l = \left[\frac{\partial\varepsilon_l}{\partial E_g}\left(\frac{\partial E_g}{\partial F}\right) + \frac{\partial\varepsilon_l}{\partial\Gamma}\left(\frac{\partial\Gamma}{\partial F}\right) + \frac{\partial\varepsilon_l}{\partial I}\left(\frac{\partial I}{\partial F}\right)\right]\Delta F, \quad (l=1,2) \tag{4}$$

where E_g is the critical energy, Γ the broadening parameter, and I the intensity of the excitonic transition.[15–18] The spectral form of the dielectric function is modeled by a Lorentzian absorption profile

$$\varepsilon = \varepsilon_1 + i\varepsilon_2 = 1 + \frac{I}{E_g - E - i\Gamma}. \tag{5}$$

Since the modulation of ε_1 dominates at the peaks A and B, as discussed above, their PR spectra are

$$\begin{aligned}\frac{\Delta R}{R} &\propto \frac{\partial\varepsilon_1}{\partial E_g}\left(\frac{\partial E_g}{\partial F}\right) + \frac{\partial\varepsilon_1}{\partial\Gamma}\left(\frac{\partial\Gamma}{\partial F}\right) + \frac{\partial\varepsilon_1}{\partial I}\left(\frac{\partial I}{\partial F}\right) \\ &\propto \left(\frac{\partial E_g}{\partial F}\frac{I}{\Gamma^2}\right)\frac{1-y^2}{(1+y^2)^2} + \left(\frac{\partial\Gamma}{\partial F}\frac{I}{\Gamma^2}\right)\frac{2y}{(1+y^2)^2} \\ &\quad - \left(\frac{\partial I}{\partial F}\frac{1}{\Gamma}\right)\frac{y}{1+y^2},\end{aligned} \tag{6}$$

where $y=(E-E_g)/\Gamma$. It is noted that the three line shape factors $(1-y^2)/(1+y^2)^2$, $2y/(1+y^2)^2$, and $y/(1+y^2)$, depend merely on E_g and Γ.[15] Five free parameters including E_g, Γ, and three bracketed coefficients $[(\partial E_g/\partial F)I/\Gamma^2$, $(\partial\Gamma/\partial F)I/\Gamma^2$, and $(\partial I/\partial F)1/\Gamma]$ in Eq. (6) are used to integrate the three line shape factors into the PR curve in the fitting, where E_g and Γ determine the line shape factors, while the bracketed coefficients give rise to their relative contributions. Shown in Figs. 3(a) and 3(b) are the least-squares fitting results for A and B, which are in excellent agreement with the experiment. The extracted energy gap and the broadening are 1.403 ± 0.001 eV and 0.005 ± 0.001 eV for A, and 2.114 ± 0.001 eV and 0.023 ± 0.001 eV for B, which are listed in Table I. The bracketed coefficients obtained can suggest which modulation factor (critical energy or broadening or pumping intensity modulation) the PR mainly arises from. For example, their relative magnitude 63:3:1 for A indicates that the PR here is governed by the energy gap modulation.

For the transition A', the PR spectrum becomes

$$\begin{aligned}\frac{\Delta R}{R} &\propto \frac{\partial\varepsilon_2}{\partial E_g}\left(\frac{\partial E_g}{\partial F}\right) + \frac{\partial\varepsilon_2}{\partial\Gamma}\left(\frac{\partial\Gamma}{\partial F}\right) + \frac{\partial\varepsilon_2}{\partial I}\left(\frac{\partial I}{\partial F}\right) \\ &\propto \left(\frac{\partial E_g}{\partial F}\frac{I}{\Gamma^2}\right)\frac{2y}{(1+y^2)^2} + \left(\frac{\partial\Gamma}{\partial F}\frac{I}{\Gamma^2}\right)\frac{y^2-1}{(1+y^2)^2} \\ &\quad + \left(\frac{\partial I}{\partial F}\frac{1}{\Gamma}\right)\frac{1}{1+y^2},\end{aligned} \tag{7}$$

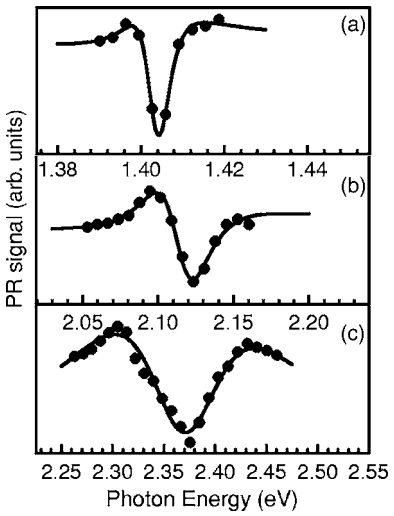

FIG. 3. The first derivative fitting for the PR (a) peak A, (b) peak B, and (c) peak A'. The dots are the experimental data and the lines are the fitted curves.

where $y=(E-E_g)/\Gamma$. Likewise, three line shape factors from the derivatives $\partial\varepsilon_2/\partial E_g$, $\partial\varepsilon_2/\partial\Gamma$, and $\partial\varepsilon_2/\partial I$ are fitted into the experimental PR with five free parameters used. As shown in Fig. 3(c), there is a good agreement between the experimental data and the fitting curve. E_g and Γ obtained for A' are 2.367 ± 0.004 eV and 0.072 ± 0.004 eV, respectively, and the larger broadening is just as expected from the broader minor peak of ε_2 for the (5, 0) tube, which can be seen in Fig. 2(b).

By comparing the energies of the critical points in the measured absorption, PR and the calculated imaginary parts ε_2 of the dielectric functions, we find that the results of the absorption and the PR are of excellent consistency. However, they differ from the LDA calculation by a large blueshift for A and B but a slight blueshift for A' in energies, indicated in Table I. The difference cannot be only attributed to the need of self-energy correction for the LDA bands, as pointed out by Spataru *et al.*[8] The excitonic and many-electron effects must also be considered to account for the discrepancy, since Coulomb interaction cannot be neglected in this 1D system. Previous research[4–6] has found that Coulomb interaction in SWNTs gives rise to both an increase of the band gap and an enhancement of the exciton binding energy. In fact, the optical transition energy is not accurately determined in the calculation until considering of whether the Coulomb interaction is governed by the attractive or repulsive term in a specific tube.[8] Our experimental results imply that the repulsive Coulomb interaction dominates in the (4, 2) and (5, 0)

TABLE I. Transition energies at critical points of the SWNTs from LDA calculation, absorption, and PR measurement.

Critical points	A (eV)	B (eV)	A' (eV)
LDA calculation	1.1	1.9	2.3
Absorption	1.37	2.1	—
PR	1.403	2.114	2.367

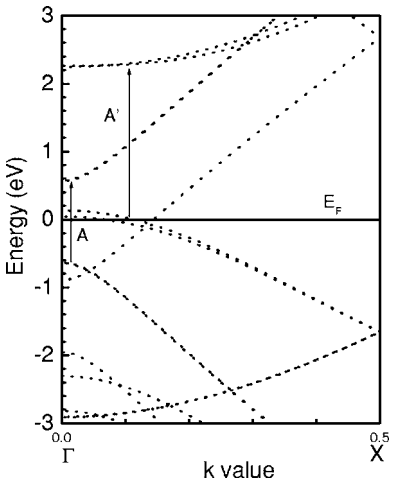

FIG. 4. The band structure for the (5, 0) tube calculated by Liu and Chan (Ref. 3). The optical transitions corresponding to A and A' are indicated by the arrows. The Fermi level E_F is at 0.

tubes, which leads to the blueshift of the transition energies A and B from the experiments with respect to from the LDA calculation. The shift of the higher energy peak A' appears to be very small in contrast with the two fundamental transitions A and B. This is presumably because the larger exciton binding energy in the higher energy bands almost compensates the repulsive-interaction-induced blueshift. We notice that Ichida *et al.*[5,6] have observed the same phenomena that the shift of the higher energy transition is much smaller than that of the lowest transition in SWNTs.

It is noted that the PR signal at A' is much stronger than at A and B, in contrast to the trace of the absorption spectrum where A' is unobservable among the neighboring broad absorption features. This contrast can come from two possibilities: one is the nearly resonant excitation of the transition A' in the PR case, another one is the natural difference between the absorption and the derivativelike modulated reflectance. For the absorption, the intensity is only determined by the initial states (valence bands) occupation and the oscillator strength; for the PR, it is related to the variation of the occupation of the associated density of states. It is seen from the band structure (Fig. 4) calculated by Liu and Chan,[3] that the transition A' corresponds to the excitation of the electrons from the crossing of the Fermi level and the valence band, to its optical permitted higher conduction band in the (5, 0) tube. At the Fermi level, it is obvious that the modulation will be the most sensitive due to the fact that the variation of the occupation of states near the Fermi level is always very large. This benefits the observation of the A' in the PR spectrum, rather than in the absorption spectrum.

IV. CONCLUSION

In conclusion, the modulated reflectance spectrum has been measured for the 0.4-nm carbon nanotubes grown within zeolite template, and the results are in good agreement with the absorption measurement and the LDA calculation after Coulomb interactions are considered. The convolution of many characteristics in the absorption spectrum is removed in the photoreflectance measurement, and all van Hove singularities become clear and well-recognized. It is another strong evidence for the peculiar band structures of the existed narrowest carbon nanotubes.

ACKNOWLEDGMENTS

This work is supported by RGC grant No. HKUST6057/02P. The authors are grateful to the support from Professors C. T. Chan and B. A. Foreman and J. T. Ye of this department.

*Corresponding author. Electronic address: phweikun@ust.hk

[1] N. Wang, Z. K. Tang, G. D. Li, and J. S. Chen, Nature (London) **408**, 50 (2000).
[2] Z. M. Li, Z. K. Tang, H. J. Liu, N. Wang, C. T. Chan, R. Saito, S. Okada, G. D. Li, J. S. Chen, N. Nagasawa, and S. Tsuda, Phys. Rev. Lett. **87**, 127401 (2001).
[3] H. J. Liu and C. T. Chan, Phys. Rev. B **66**, 115416 (2002).
[4] T. Ando, J. Phys. Soc. Jpn. **66**, 1066 (1997).
[5] M. Ichida, S. Mizuno, Y. Tani, Y. Saito, and A. Nakamura, J. Phys. Soc. Jpn. **68**, 3131 (1999).
[6] M. Ichida, S. Mizuno, Y. Saito, H. Kataura, Y. Achiba, and A. Nakamura, Phys. Rev. B **65**, 241407(R) (2002).
[7] T. G. Pedersen, Phys. Rev. B **67**, 073401 (2003).
[8] C. D. Spataru, S. Ismail-Beigi, L. X. Benedict, and S. G. Louie, Phys. Rev. Lett. **92**, 077402 (2004).
[9] P. Y. Yu and M. Cardona, *Fundamentals of Semiconductors: Physics and Materials Properties*, 3rd ed. (Springer, Berlin, 2001).
[10] F. H. Pollak and H. Shen, Mater. Sci. Eng., R. **10**, 275 (1993).
[11] R. E. Nahory and J. L. Shay, Phys. Rev. Lett. **21**, 1569 (1968).
[12] H. J. Liu, Z. M. Li, Q. Liang, Z. K. Tang, and C. T. Chan, Appl. Phys. Lett. **84**, 2649 (2004).
[13] J. Guo, C. Yang, Z. M. Li, M. Bai, H. J. Liu, G. D. Li, E. G. Wang, C. T. Chan, Z. K. Tang, W. K. Ge, and X. Xiao, Phys. Rev. Lett. **93**, 017402 (2004).
[14] B. O. Seraphin and N. Bottka, Phys. Rev. **145**, 628 (1966).
[15] B. V. Shanabrook, O. J. Glembocki, and W. T. Beard, Phys. Rev. B **35**, 2540 (1987).
[16] W. M. Theis, G. D. Sanders, C. E. Leak, K. K. Bajaj, and H. Morkoc, Phys. Rev. B **37**, 3042 (1988).
[17] T. S. Moss, *Handbook on Semiconductors*, Vol. 2 (Elsevier Science, Amsterdam, 1992).
[18] D. G. Seiler and C. L. Littler, *The Spectroscopy of Semiconductors* (Academic Press, Boston, 1992).